



Published in final edited form as:

Neuroimage. 2007 April 15; 35(3): 1201–1210. doi:10.1016/j.neuroimage.2007.01.024.

Mapping the spinal and supraspinal pathways of dynamic mechanical allodynia in the human trigeminal system using cardiac-gated fMRI

Caterina Mainero^{*}, Wei-Ting Zhang^{*}, Ashok Kumar, Bruce R. Rosen, and A. Gregory Sorensen

MGH/MIT/HMS Athinoula A. Martinos Center for Biomedical Imaging, Massachusetts General Hospital, Charlestown, MA, & Harvard Medical School, Boston, MA

Abstract

Following injury and inflammation, pain to light stroking (dynamic mechanical allodynia) might develop at the damaged site (primary area) or in adjacent normal tissue (secondary area).

Using fMRI we mapped changes in the spinal trigeminal nucleus (spV), and supraspinal brainstem nuclei following heat/capsaicin-induced primary and secondary dynamic mechanical allodynia in the human trigeminal system. The role of these structures in dynamic mechanical allodynia has not been clarified yet in humans. During the control session we applied the same mechanical stimuli to the same untreated trigeminal area.

Primary and secondary mechanical allodynia showed equal levels of perceived pain intensity, and compared to control mechanical stimulation exhibited similar responses in the ipsilateral spV and contralateral ventrolateral periaqueductal gray (vlPAG). Activity in the spV was significantly higher during both conditions versus the control mechanical stimulation, indicating that central sensitization of second-order neurons is similar for primary and secondary mechanical allodynia. The vlPAG showed decreased activity that inversely correlated with pain ratings during primary allodynia, i.e. the more deactivated the vlPAG the higher the pain intensity ($p < 0.05$, Pearson's correlation).

Primary and secondary dynamic mechanical allodynia were also characterized by significant differences involving distinct supraspinal structures mainly involved in pain modulation and including the rostroventromedial medulla, pons reticular formation, dorsolateral PAG, all more active during primary versus secondary allodynia, and the medial reticular formation of the caudal medulla that was more active during secondary versus primary allodynia. These results indicate the pain modulatory system is involved to a different extent during primary versus secondary mechanical allodynia.

© 2007 Elsevier Inc. All rights reserved.

Correspondence should be addressed to: Caterina Mainero, MD, Ph.D, Athinoula A. Martinos Center for Biomedical Imaging, Massachusetts General Hospital, Harvard Medical School, Bldg 149 (2301), 13th Street, Charlestown, MA 02129. Tel. 1-617-724-7746, Fax. 1-617-726-7422, Email: caterina@nmr.mgh.harvard.edu.

^{*}These authors contributed equally to this work.

Publisher's Disclaimer: This is a PDF file of an unedited manuscript that has been accepted for publication. As a service to our customers we are providing this early version of the manuscript. The manuscript will undergo copyediting, typesetting, and review of the resulting proof before it is published in its final citable form. Please note that during the production process errors may be discovered which could affect the content, and all legal disclaimers that apply to the journal pertain.

Keywords

fMRI; allodynia; mechanical; brainstem; pain modulation

Introduction

Allodynia (pain to innocuous stimuli) typically follows inflammation and injury to extraneural or neural tissue. Under these conditions peripheral nociceptors become sensitized and spinal second-order neurons can increase their excitability (central sensitization) (Woolf and King, 1990). The perception of allodynia is selective to the sensory modality tested (thermal, mechanical), and to the area examined (primary, secondary). Allodynia to gentle stroking (dynamic mechanical allodynia) develops both at the site of damage (primary area) and in adjacent normal tissue (secondary area) (Koltzenburg, et al., 1992, Ali, et al., 1996), and represents one of the most distressing symptoms of neuropathic pain.

Although it is generally thought that the mechanisms of primary and secondary allodynia are, respectively, peripheral and central, some authors have hypothesized the existence of central mechanisms in the development of dynamic mechanical allodynia in the primary area (Woolf and King, 1990, Simone, et al., 1991, Koltzenburg, et al., 1992). They also speculated that similar spinal mechanisms might operate in this form of allodynia regardless of being in the primary or secondary area (Koltzenburg, et al., 1992).

Animal data suggest that a significant contribution to the development and maintenance of mechanical allodynia comes from the descending pain modulatory system including the periaqueductal gray (PAG), rostroventromedial medulla (RVM) and adjacent reticular formation (Porreca, et al., 1999, Urban and Gebhart, 1999, Vanegas and Schaible, 2004), through either inhibitory or excitatory influences. The role of these structures, however, is not without controversies: descending inhibition and facilitation can be simultaneously triggered and the predominance of one effect over the other seems different depending on the area tested (primary, secondary) (Vanegas and Schaible, 2004).

While the cortical correlates of dynamic mechanical allodynia have been disclosed in humans by previous neuroimaging studies (Iadarola, et al., 1998, Witting, et al., 2001, Maihofner, et al., 2004, Schweinhardt, et al., 2006), *in vivo* mapping of changes in the spinal second-order neurons and supraspinal brainstem nuclei during primary and secondary dynamic mechanical allodynia is lacking due to the technical difficulties involved in the imaging of these areas. fMRI studies of the brainstem during pain have only recently started to emerge (DaSilva, et al., 2002, Dunckley, et al., 2005, Zambreanu, et al., 2005), and we have demonstrated that triggering fMRI acquisition phase locked to a particular time point of the subject's cardiac cycle (cardiac-gated fMRI) significantly increases the detection rate of fMRI activation in the brainstem (Zhang, et al., 2006).

Using cardiac-gated fMRI, we mapped activity in the spinal trigeminal nucleus (spV) and pain modulatory structures in the brainstem and above following heat/capsaicin-induced dynamic mechanical allodynia in the human trigeminal system (Petersen and Rowbotham, 1999). First we assessed whether and which plastic neuronal changes of nociceptive transmission occur in spinal and supraspinal brainstem sites during primary and secondary mechanical allodynia. Secondly, we compared brainstem responses to mechanical stimuli to the secondary area with those following the same stimuli to the primary area, possibly disclosing differences in central processing between the two conditions.

These findings could have important implications as the heat/capsaicin model shares typical characteristics with clinical neuropathic pain, and the area of secondary mechanical allodynia induced by this model reflect, at least in part, the mechanisms that might contribute to allodynia in neuropathic pain disorders.

Materials and Methods

Subjects

Twelve healthy male subjects (11 right-handed; mean \pm SD age of 26.6 \pm 6.2 years) participated in the study. The left-handed subject was not excluded because we did not detect any difference in the laterality of his fMRI results compared to the other subjects.

None of the subjects was suffering from any form of acute or chronic pain, or was taking drugs able to interfere with itch or pain sensations and flare responses (i.e. analgesics, antihistamines, calcium or sodium channel blockers) or benzodiazepines, antidepressants, and opioids. All subjects were instructed not to consume caffeine beginning the night before the experiment.

Informed consent form was obtained from all subjects prior study entry, and the study procedures were approved by the Institutional Review Board of our Institution.

Experimental allodynia

Dynamic mechanical allodynia was induced to the right ophthalmic division (V1) of trigeminal nerve using the heat/capsaicin sensitization model (Petersen and Rowbotham, 1999). In each subject we first marked the treatment site on the right V1 (1.6 cm²). The premarked skin was then heated for 5 minutes at 45°C using a 1.6 cm² Peltier thermode (Medoc, Haifa Israel) after which 0.1% of capsaicin cream (Capzasin-HP, Chattem, Inc, USA) was applied over the same area for other 30 minutes. The area of capsaicin application was covered with a Tegaderm tape to avoid spreading of the cream outside the premarked borders. Subjects rated the perceived intensity to the initial contact stimulation (45°C) using a Numerical Rating Scale (NRS) ranging from 0 (no pain) to 10 (highest pain imaginable). The same scale was applied to rate the pain elicited by the topical capsaicin application every 10 minutes. After capsaicin removal, the borders of the area of secondary dynamic mechanical allodynia were delineated by stimulating with a brush along four linear paths parallel and vertical to the midline of the face from distant points toward the application site, until the subject reported unpleasant sensations. These borders were then marked on the skin, and the area of allodynia was then calculated ($D/2 \times d/2 \times \pi$; where D and d represent the horizontal and vertical diameters of the area).

fMRI study

fMRI data were acquired on a 3T system (Siemens Trio, Erlangen, Germany) using an eight-channel head array coil. Each subject lay supine in the scanner with eyes closed. All subjects were randomly assigned to one of two counterbalanced groups to undergo two fMRI sessions, separated by an interval of at least a week, one during innocuous brush to the right V1 immediately after heat/capsaicin-induced allodynia (heat/capsaicin session), and one during the same stimuli to the untreated right V1 (control session). The order of the two sessions was randomized. The study design is illustrated in Fig. 1.

To eliminate the effect of pulsatile brainstem motion, we synchronized fMRI acquisition to a particular phase of the subject's cardiac cycle (Guimaraes, et al., 1998). The ECGR-wave was used to trigger the fMRI measurement, and the exact triggering time could be read from the internal clock of the scanner. Therefore the intervals between two consecutive

measurements could be calculated and T1 differences based on variations in the R-R interval corrected for.

During each fMRI study, 17 sagittal slices ($3 \times 3 \times 3 \text{ mm}^3$, gap 20%) were acquired sequentially (right to left) every three heartbeats (TR~3 s) with a gradient EPI sequence (TE 30 ms; flip angle 90° ; in-plane matrix 64×64 ; FOV $192 \times 192 \text{ mm}^2$). The acquisition window was 1000 ms and there was an adjustable delay (~2000 ms) to ensure that the next trigger came after two other heartbeats. There was no delay between the trigger signal and the image acquisition. Seventeen sagittal slices allowed a full coverage of the brainstem and thalamus. Parallel acceleration technique (iPAT) with GRAPPA (generalized auto-calibrating partially parallel acquisition) reconstruction was used with an acceleration factor of 2. T1-weighted EPI images (TR 14 s; TE 39 ms; in-plane matrix 64×64 ; FOV $200 \times 200 \text{ mm}^2$) in the same slice prescription but covering the whole brain (41 slices) were also acquired for the purpose of image co-registration. High resolution isotropic T1-weighted anatomical scans (TR 2530 ms; TE 3.4 ms; in-plane matrix 256×256 ; $1 \times 1 \times 1 \text{ mm}^3$) were also acquired for superimposition of fMRI activation maps.

Sensory stimulation

Mechanical stimulation was delivered using a soft natural bristle brush (1.0 cm diameter) pivoting at its mid-point on a stabilized base and forming a lever. The brush was manipulated from outside the scanner by means of two cables attached on each side of the lever. The assembly transduced the alternating horizontal forces applied to the cables by the operator outside the scanner into a lateral force on the forehead of the subject inside the scanner (measured force 0.3 N/cm^2).

Innocuous brush stimuli were applied to the premarked areas of interest (normal skin; primary and secondary areas of dynamic mechanical allodynia) on the right V1 with a frequency of 2 Hz. Brush stimuli were applied four times each for 30 s, alternating four intervals of rest lasting 30 s. During the heat/capsaicin session brush stimuli were applied to either the primary or secondary area in a random order.

Immediately following each fMRI scan, subjects rated the perceived intensity of the received mechanical stimuli on a 0 (no pain) to 10 (highest pain imaginable). The pain ratings were compared with one-way ANOVA with post Bonferroni test between the untreated, primary, and secondary area. A post-scan interview was performed to confirm that there was no ongoing baseline pain during the scanning.

Data analysis

Analysis of fMRI images to identify regions with significant stimulus-correlated changes in BOLD (blood oxygen level dependent) signal was performed in a multi-stage process using the package AFNI (Cox, 1996) and in-house programs. The EPI data were first motion-corrected. Since heart rate typically fluctuates, the interimage time with cardiac gating also fluctuates from image to image. T1 correction was then necessary to correct changes in signal intensity due to different residual longitudinal magnetization following variability in TR. This correction was performed using the method proposed by Guimaraes et al (Guimaraes, et al., 1998), according to which T1 in each voxel was fitted using different intervals between measurements and the corresponding measured signal; signal intensity was then corrected to the averaged TR.

The T1-corrected data were then spatially smoothed using a Gaussian kernel of 4 mm full-width at half-maximum, low- and high-pass filtered (1/120 Hz). Statistical analysis was performed using a two-stage approach. First, stimulus input for statistical analysis was convolved with gamma function, incorporating the hemodynamic delay, to estimate the

hemodynamic response function. This function was then over-sampled with 0.1 s interval and down-sampled again irregularly to reflect the different TRs between the measurements. Regression analysis was performed with 3dDeconvolve in AFNI to calculate regression coefficients and corresponding *t* statistics.

For group analysis, individual statistical maps and anatomical data were transformed into Talairach space, and functional data were resampled to $3 \times 3 \times 3 \text{ mm}^3$. We then used a mixed (fixed- and random-effect) model. Regression coefficients of the same stimuli but in different conditions (brush to normal skin, primary and secondary area) were compared with two-way ANOVA with different conditions as a fixed factor and subjects as a random factor. Four output contrasts were generated: 1) brush to the untreated skin versus rest (control mechanical stimulation), 2) brush to the primary and 3) secondary area versus control mechanical stimulation 4) brush to the secondary area versus the primary area.

For group maps we used a *p* value of 0.05 corrected for multiple comparisons according to the Monte Carlo simulation method, a minimum cluster size of three voxels (81 mm^3), and a *T* value > 2.05 .

All high resolution anatomical scans were transformed into Talairach space and averaged; each individual transformed anatomical image was then anatomically compared to the averaged one by visual inspection to confirm the absence of gross variation in the alignment of the lower brainstem (pons and medulla). Brainstem outlines of all subjects are shown in Fig. 2.

Group activation maps were overlaid on a representative Talairach transformed anatomical image, and the maximum *t* values and *x*, *y*, *z* coordinates of significantly activated areas were reported (Talairach and Tournoux, 1988). To exclude partial volume effects, clusters significantly activated at group analysis were also checked on the individual fMRI data.

Localization of brainstem activation

We used a landmark-based topographical approach previously described (DaSilva, et al., 2002) to identify the location of the activation clusters in the lower brainstem (medulla and pons). According to this method the brainstem can be parcellated into six parcellation units (PUs) in the midbrain, four PUs in the pons, and four in the medulla. This method has been successfully adopted to identify somatotopic activation within the spinal trigeminal nucleus (spV) during noxious heat. The spV is located in the dorsolateral portion of the brainstem, and extend from the upper cervical cord/caudal medulla to the rostral pons (Young and Perryman, 1984). In our study, because we only stimulated V1 we did not attempt to characterize the somatotopic subdivisions of the spV.

Tactile modalities from healthy skin of the face are encoded by low-threshold mechanosensitive A β afferents with large myelinated axons that synapse directly in the principal sensory nucleus (PSN). To identify this nucleus in the ipsilateral dorsal pons, we encompassed two slices above, two slices below, and the slice in which trigeminal roots traverse. The parcellation method in the pons was used to distinguish the anterior PUs that correspond to the basal pons and contain the pontocerebellar fibres and descending corticospinal tract from the posterior PUs that contain the remaining structures and fourth ventricle and that correspond to the pontine tegmentum.

Identification of activation clusters in the midbrain was based on the Talairach atlas and on other anatomical landmarks including the superior and inferior colliculi, the cerebral aqueduct, the pontomesencephalic junction, the posterior commissure and the midline. The parcellation method in the midbrain was used to distinguish the most anterior part that

contains crus cerebri and substantia nigra, from the middle PU (midbrain tegmentum), and posterior PU (midbrain tectum). Sketches and micrographs adapted from the atlas of Duvernoy (1995) were also used to help identify the location of activation clusters (Duvernoy, 1995).

Results

Psychophysics

All subjects except one reported moderate pain to either contact heat (45°C) or capsaicin application. This subject was therefore classified as “non responder” and excluded from group analyses. The mean \pm SE perceived pain intensity to the initial contact heat (45°C) stimulation was 4.6 ± 0.5 . The mean \pm SE pain averaged during the 30 minutes of topical capsaicin application was 5.2 ± 0.7 , and it positively correlated ($p = 0.02$, by Pearson’s correlation) with the area of dynamic mechanical allodynia (mean \pm SE: $10.9 \pm 1.7 \text{ cm}^2$ including the primary area) induced by heat/capsaicin application.

All subjects rated brush stimulation to the untreated skin as 0. During the heat/capsaicin fMRI session, subjects reported a change in the quality of the sensation to brush stimuli to either the primary or adjacent area defined as “unpleasant”. Overall the pain ratings (mean \pm SE) were significantly higher during mechanical stimulation of either primary (1.6 ± 0.4) or secondary area (1.3 ± 0.4) compared to the normal skin ($p < 0.01$). We did not find significant differences in pain ratings to mechanical stimulation between the primary and secondary area.

fMRI

Control mechanical stimulation—Group analysis of innocuous brush stimulation to the untreated skin on the right V1 showed significant activation in the contralateral caudate and cingulate cortex (CC, BA 24), in the ipsilateral putamen and anterior insula. This pattern of activation during light brush to healthy subjects has been described previously (Davis, et al., 1998, Iadarola, et al., 1998). At a lower level of significance (uncorrected $p < 0.01$, Talairach x, y, z coordinates: 5, -23, -29) we found activation in the ipsilateral dorsal pons in an area corresponding to the principal sensory nucleus (PSN) where, under normal conditions, low-threshold mechanosensitive A β afferents encoding tactile modalities from healthy skin of the face synapse.

Brush to either the primary or secondary area versus control mechanical stimulation

The comparison analysis of activation maps during mechanical stimulation to the primary area and during control mechanical stimulation showed that brush to the primary area induced an increased activity in the ipsilateral caudal dorsal medulla/upper cervical cord in an area anatomically corresponding to the spV, in the rostral medulla in an area consistent with the location of the RVM, in the dorsal reticular formation of the pons and in the contralateral dorsolateral (dl) PAG (Table 1, Fig. 3A). Activation in the pons was consistent with the location of the locus coeruleus (LC) and parabrachial nucleus (PBN).

Like primary mechanical allodynia, secondary mechanical allodynia was also associated with a greater activity in the ipsilateral caudal dorsal medulla/upper cervical cord compared to the mechanical control stimulation. Decreased activity in the contralateral ventrolateral (vl) PAG was also detected (Table 1, Fig. 3B). At a lesser level of significance (uncorrected $p < 0.001$) we found activation of a small cluster of the dorsomedial pons, consistent with the location of the pons reticular formation.

Other supra-brainstem foci of increased activity during either primary or secondary mechanical allodynia compared to the mechanical control stimulation are shown in Table 1.

Brush to the secondary area versus brush to the primary area—The comparison of brush to the area of secondary dynamic mechanical allodynia versus the same stimulus to the area of primary mechanical allodynia yielded significant differences in different brainstem and higher regions despite similar levels of perceived pain intensity (Table 2, Fig. 4).

In the brainstem, primary dynamic mechanical allodynia showed more activity in the RVM, in a region of the contralateral PRF (where LC and PBN are located), and in the bilateral dlPAG (all in blue in Fig. 4). In contrast, brush to the secondary area versus the primary area determined a significantly higher fMRI activity in the medial part of the caudal medulla consistent with the reticular formation.

Two brainstem regions were eliminated by this analysis: the ipsilateral spV and the contralateral vlPAG. The finding in the spV was not surprising as both primary and secondary dynamic mechanical allodynia showed increased activity in this brainstem region compared to the control mechanical stimulation. More surprising was the result in the vlPAG. However, by examining the fMRI maps of primary mechanical allodynia in the vlPAG, we also found that there was a tendency towards a subthreshold decreased (negative) activity as observed during secondary mechanical allodynia.

To investigate the relationship between fMRI activity in these brainstem areas eliminated by removing the pain intensity component and pain ratings, we outlined on the high-resolution T1-weighted structural scans regions of interest (ROI) centered on the spV and vlPAG. The definition of those ROIs was performed with the help of a detailed atlas of the brainstem (Duvernoy, 1995). The ROIs were then transformed into Talairach space and these transformed masks were applied to each subject's activations, also in Talairach space, to determine the mean signal change. This method allowed us to take into account any subtle variation in the anatomy between subjects. The correlation between the mean signal change in each ROI and pain ratings during either primary or secondary mechanical allodynia was assessed using Pearson Correlation. We found a significant negative correlation between the mean signal change in the vlPAG and pain ratings during mechanical stimulation of the primary area ($p < 0.05$, Pearson's correlation coefficient = -0.6 , Fig. 5).

We also compared the mean signal change in the ROIs of spV and vlPAG during primary mechanical allodynia versus secondary mechanical allodynia, and we did not find any significant difference ($p < 0.14$ by Student's paired t test, two-tailed). However, we found significant increase in the mean signal change in the spV when we compared primary or secondary allodynia versus control mechanical stimulation ($p < 0.0001$ and $p < 0.04$ respectively by ANOVA with post Bonferroni test). These ROI-based results in the spV and vlPAG were consistent with our voxel-based group analysis results.

Discussion

Using cardiac gated fMRI we mapped *in vivo* changes in brainstem nuclei during primary and secondary dynamic mechanical allodynia in the human trigeminal pathway.

The intensity of the perceived pain was similar across primary and secondary skin areas. The subtraction of the fMRI changes during primary mechanical allodynia to those during secondary allodynia allowed us to disclose differences in brainstem central processing between the two conditions not related to the perceived pain intensity.

Primary and secondary dynamic mechanical allodynia versus control mechanical stimulation

Spinal level (spV)—Following heat/capsaicin application to the right V1 dynamic mechanical allodynia occurred at the site of injury, and in adjacent normal skin; in both cases it was associated with increased fMRI activity in the spV, suggesting central sensitization of second-order neurons.

It has been demonstrated that dynamic mechanical allodynia in either the primary or secondary area is not mediated by nociceptors but by input of low thresholds A β afferents that normally signal light touch, not pain (Lindblom and Verrillo, 1979, Koltzenburg, et al., 1992, Torebjork, et al., 1992, Ochoa and Yarnitsky, 1993, Ossipov, et al., 1999). In normal conditions, A β fibers conveying tactile stimuli from the forehead synapse in the PSN in the pons. Because excitability increases of spinal second-order neurons have been repeatedly observed in animals following tissue injury, inflammation or chemical irritants (McMahon and Wall, 1984, Cook, et al., 1987, Woolf and King, 1990, Simone, et al., 1991), it has been proposed that prolonged or intense C-nociceptor activation leads to changes in central processing such that nociceptive dorsal horn neurons (i.e. spV in our study) show enhanced responses to A β low threshold mechanoreceptors (central sensitization) (Simone, et al., 1989, Woolf and King, 1990, Woolf, et al., 1994).

We provide the first objective evidence of this phenomenon in humans by mapping during dynamic mechanical allodynia *in vivo* plastic changes in the spV that likely reflect central sensitization of second-order neurons. Furthermore both the voxel-based and the ROI-based group analyses showed that similar changes in the spV occurred during brush stimulation in either the primary or secondary area..

Supraspinal brainstem level (RVM, PRF, PAG)—The areas of primary and secondary dynamic mechanical allodynia show partly common partly different patterns of activation in supraspinal brainstem structures compared to the control mechanical stimulation. In both conditions we found increased activity in the dorsal PRF that corresponded anatomically with the location of the LC and PBN, and adjacent dorsal reticular nuclei during primary dynamic mechanical allodynia, while it involved only a small part of the medial dorsal PRF during secondary dynamic mechanical allodynia.. The pontine activation we found, especially in the PBN and in LC, could be the result of two distinct mechanisms that not necessarily are in contrast with each other but could rather operate at the same time: 1) processing of ascending nociceptive information; 2) descending pain modulation. The PBN is well known to participate in ascending nociception through the spinoparabrachial pathways (Hunt and Mantyh, 2001) as well in pain modulation through a spino-bulbo-spinal pathway (Suzuki, et al., 2004a). Descending projections from the LC provide an important source of pain suppression at spinal level (DeSalles, et al., 1985), but there is also evidence that LC innervation could be associated with an ascending noradrenergic system acting upon a thalamus-prefrontal cortex pain-modulation mechanism (Condes-Lara, 1998, Voisin, et al., 2005).

Primary mechanical allodynia also showed increased activity in the RVM, not observed during secondary allodynia. The RVM forms the main relay site of descending influences back to the spinal neurons, and animal studies have established a role for this structure in the development of mechanical allodynia although the RVM may show opposite effects across primary and secondary allodynic areas (Vanegas and Schaible, 2004).

Primary and secondary dynamic mechanical allodynia showed further changes to brush stimuli in two distinct regions of the PAG. Brush to the primary area versus the untreated skin determined an increased activity in the contralateral dIPAG. Conversely, during

secondary mechanical allodynia versus control mechanical stimulation we found a decreased activity of the contralateral rostral vIPAG. An ROI analysis of the mean BOLD signal change in the vIPAG showed, however, that, similarly to the secondary area, there was a tendency towards a subthreshold decreased (negative) activity also during mechanical stimulation of the primary area. The PAG is heterogeneous in terms of its cytoarchitectonic and neurochemical organization (Behbehani, 1995). The dIPAG and the vIPAG seem to have opposing roles depending on whether an animal is facing an imminent threat or a distant one: overall the dIPAG facilitates rapid autonomic and “Go” behavior such a flight or aggression (Beckett, et al., 1992, Beckett and Marsden, 1997, Jacob, et al., 2002), while microstimulation of the vIPAG results in sympathetic inhibition and passive behavior (Bago and Dean, 2001, Odeh, et al., 2003). In this context the increased activation of the dIPAG during primary and not secondary mechanical allodynia could reflect an increased response towards the presence of an imminent threat represented by the area of actual damage (primary area).

Higher order structures—Our results of activations in higher order structures are consistent with previous studies during dynamic mechanical allodynia in humans (Iadarola, et al., 1998, Petrovic, et al., 1999, Witting, et al., 2001, Maihofner, et al., 2003, Schweinhardt, et al., 2006). The primary and secondary somatosensory cortices were not covered due to the partial brain acquisition.

We document increased activity in the cerebellum during both primary and secondary allodynia. Cerebellar activations have been frequently described during painful stimuli, and have been often attributed to the intention to perform motor responses or withdrawal (Iadarola, et al., 1998). However, there is evidence that the cerebellum might also modulate nociception through its connections with the medullary dorsal reticular nucleus (Saab and Willis, 2003)

We also document an increased activity in the amygdala during both primary and secondary dynamic mechanical allodynia. The amygdala, together with the prefrontal and anterior cingulate cortex, is involved in pain modulation through a PAG link to the brainstem (Fields, 2000). This connects our findings to the well characterized aversive dimension of allodynic pain.

Differences between the primary and secondary areas of dynamic mechanical allodynia

The areas of primary and secondary dynamic mechanical allodynia yielded several significant differences when compared to each other. These differences were not related to the perceived pain intensity, as pain ratings did not significantly differ between the two conditions.

The spV and vIPAG were the only two brainstem areas eliminated by the subtraction analysis. This might be due to the similarities in central sensitization in the spV between primary and secondary mechanical allodynia, and to the removal of the pain intensity component for the vIPAG. We found that the mean signal change in this region of the PAG inversely correlated with pain scores during stimulation of the primary area, i.e. the more deactivated in the vIPAG the higher the intensity of the perceived pain. Electrical stimulation of the vIPAG produces analgesia in both animals and humans, and can reduce mechanical and cold allodynia in animal models of neuropathic pain (Pertovaara, et al., 1997, Lee, et al., 2000). It has been shown that activation in the PAG may increase during a distraction condition, and the total increase in activation is predictive of changes in perceived pain intensity (Tracey, et al., 2002). In our study, the reduced activity in the vIPAG following heat/capsaicin sensitization could reflect decreased descending inhibition of pain, at least for the primary area.

Overall secondary mechanical allodynia compared to primary allodynia was characterized by differences at the supraspinal level. These changes consisted in increased activity during secondary versus primary allodynia in a cluster localized in the reticular formation of the medial part of the caudal medulla, and in greater fMRI activity during primary versus secondary allodynia in other supraspinal brainstem regions of the pain matrix including the RVM, the lateral part of the contralateral PRF (where the locus coeruleus is located), the bilateral PAG, but in the dorsolateral part.

The RVM, PRF and dlPAG have a well established role in pain processing and modulation through a spino-bulbo-spinal loop that can either facilitate or inhibit nociceptive input at the level of the dorsal horn (Suzuki, et al., 2004b). The reticular formation in the medial caudal medulla receives afferents from different midbrain nuclei including the PAG, and is likely involved in pain modulation (Chung, et al., 1983). These results suggest that the pain modulatory structures of the brainstem are involved to a different extent during primary versus secondary dynamic mechanical allodynia.

Although BOLD fMRI does not allow the neurochemical effects of the observed changes to be elucidated (Arthurs and Boniface, 2002), it is possible that our results reflect components of inhibitory and facilitatory activity within the pain modulatory system in the brainstem. Animal studies have shown that nociception simultaneously triggers descending facilitation and inhibition, and that the predominance of one effect over the other differs depending on several factors including the area examined (primary, secondary), the experimental model used to induce allodynia, and the time of testing (Vanegas and Schaible, 2004). The differences we found between primary and secondary mechanical allodynia cannot be simply due to a “time” or “expectation” effect as we administered mechanical stimuli to the two areas in a random order.

Unlike the vlPAG, the supraspinal areas differently activated between secondary and primary mechanical allodynia, however, were not directly related to the intensity of the perceived pain. Pain, on the other hand, is not simply a sensory experience, but integrates affective, cognitive, and neurovegetative components. Top-down influences from different cortical regions (prefrontal cortex, cingulate, insula) have also been proved to play a Peiron, et al., 2000, Porro, 2003). Interestingly in our study, differences between the primary and secondary areas also involved regions above the brainstem including the medial thalamus, anterior and posterior cingulate, prefrontal cortex and the cerebellum. The primary focus of our investigation was, however, the brainstem, and due to the cardiac gated acquisition method our data on the cortical areas are limited. Future studies using cognitive/attentional tasks, as well different levels of pain stimulation could help clarifying the nature and the direction of this complex interaction between spinal-supraspinal-cortical sites. Additionally the use of more sophisticated behavioral measures, including affective ratings and degree of unpleasantness could help to better clarify differences in the perception of dynamic mechanical allodynia between primary and secondary areas, and possibly relate them to the imaging differences observed.

In conclusion, we provide a unique documentation of the *in vivo* changes in the human brainstem nuclei following experimentally-induced dynamic mechanical allodynia in the trigeminal system. We mapped changes indicative of central sensitization at the level of the second-order neurons (spV), demonstrating that they are similar for both primary and secondary mechanical allodynia. Key brainstem areas (reticular formation of medulla, RVM, PAG, PRF) involved in pain processing and modulation may play, at least in part, a different role across the damaged area and adjacent normal skin. This is in accordance with the emerging concept of pain modulation as a dynamic process that integrates nociceptive processing with multiple excitatory and inhibitory actions to adapt to the various pain

determinants. Finally we demonstrated that the rostral vIPAG is related to the intensity of the perceived allodynic pain in humans.

Acknowledgments

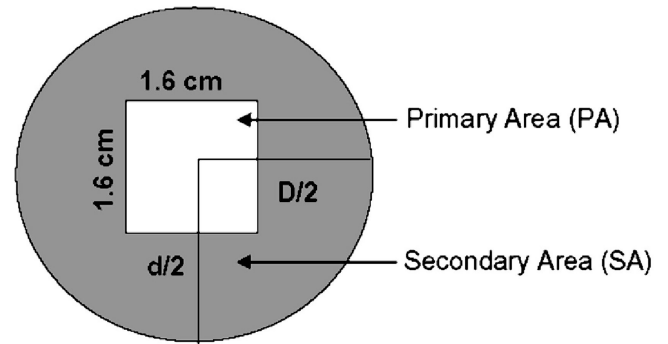
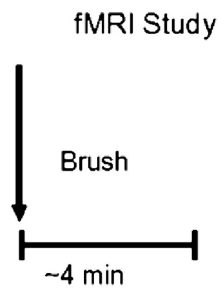
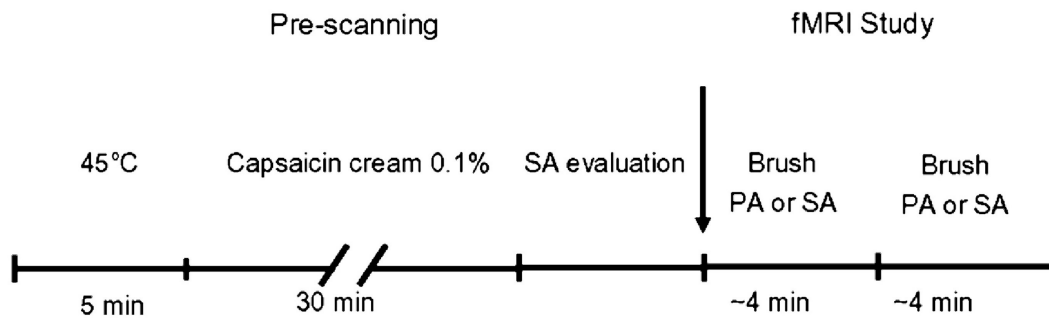
This work was supported by NIH 5P01 NS35611-07, NIH National Center for Research Resources General Clinical Resource Centers Program (M01-RR-01066), NCRR Center for Functional Neuroimaging Technologies (P41RR014075), Mental Illness and Neuroscience Discovery (MIND) Institute. We thank Mike Moskowitz and Nouchine Hadjikhani for the constructive comments. We also thank Patrick Purdon for the insightful suggestions for data analysis.

References

- Ali Z, Meyer RA, Campbell JN. Secondary hyperalgesia to mechanical but not heat stimuli following a capsaicin injection in hairy skin. *Pain* 1996;68:401–411. [PubMed: 9121830]
- Arthurs OJ, Boniface S. How well do we understand the neural origins of the fMRI BOLD signal? *Trends Neurosci* 2002;25:27–31. [PubMed: 11801335]
- Bago M, Dean C. Sympathoinhibition from ventrolateral periaqueductal gray mediated by 5-HT_{1A} receptors in the RVLM. *Am J Physiol Regul Integr Comp Physiol* 2001;280:R976–R984. [PubMed: 11247817]
- Beckett S, Marsden CA. The effect of central and systemic injection of the 5-HT_{1A} receptor agonist 8-OHDPAT and the 5-HT_{1A} receptor antagonist WAY100635 on periaqueductal grey-induced defence behaviour. *J Psychopharmacol* 1997;11:35–40. [PubMed: 9097891]
- Beckett SR, Lawrence AJ, Marsden CA, Marshall PW. Attenuation of chemically induced defence response by 5-HT₁ receptor agonists administered into the periaqueductal gray. *Psychopharmacology (Berl)* 1992;108:110–114. [PubMed: 1410130]
- Behbehani MM. Functional characteristics of the midbrain periaqueductal gray. *Prog Neurobiol* 1995;46:575–605. [PubMed: 8545545]
- Chung JM, Kevetter GA, Yeziarski RP, Haber LH, Martin RF, Willis WD. Midbrain nuclei projecting to the medial medulla oblongata in the monkey. *J Comp Neurol* 1983;214:93–102. [PubMed: 6841679]
- Condes-Lara M. Different direct pathways of locus coeruleus to medial prefrontal cortex and centrolateral thalamic nucleus: electrical stimulation effects on the evoked responses to nociceptive peripheral stimulation. *Eur J Pain* 1998;2:15–23. [PubMed: 10700297]
- Cook AJ, Woolf CJ, Wall PD, McMahon SB. Dynamic receptive field plasticity in rat spinal cord dorsal horn following C-primary afferent input. *Nature* 1987;325:151–153. [PubMed: 3808072]
- Cox RW. AFNI: software for analysis and visualization of functional magnetic resonance neuroimages. *Comput Biomed Res* 1996;29:162–173. [PubMed: 8812068]
- DaSilva AF, Becerra L, Makris N, Strassman AM, Gonzalez RG, Geatrakis N, Borsook D. Somatotopic activation in the human trigeminal pain pathway. *J Neurosci* 2002;22:8183–8192. [PubMed: 12223572]
- Davis KD, Kwan CL, Crawley AP, Mikulis DJ. Functional MRI study of thalamic and cortical activations evoked by cutaneous heat, cold, and tactile stimuli. *J Neurophysiol* 1998;80:1533–1546. [PubMed: 9744957]
- DeSalles AA, Katayama Y, Becker DP, Hayes RL. Pain suppression induced by electrical stimulation of the pontine parabrachial region. Experimental study in cats. *J Neurosurg* 1985;62:397–407. [PubMed: 3871845]
- Dunckley P, Wise RG, Fairhurst M, Hobden P, Aziz Q, Chang L, Tracey I. A comparison of visceral and somatic pain processing in the human brainstem using functional magnetic resonance imaging. *J Neurosci* 2005;25:7333–7341. [PubMed: 16093383]
- Duvernoy, HM. The human brain stem and cerebellum: surface, structure, vascularization, and three-dimensional sectional anatomy with MRI., Vol, edn. New York: Springer-Verlag Wien; 1995.
- Fields HL. Pain modulation: expectation, opioid analgesia and virtual pain. *Prog Brain Res* 2000;122:245–253. [PubMed: 10737063]

- Guimaraes AR, Melcher JR, Talavage TM, Baker JR, Ledden P, Rosen BR, Kiang NY, Fullerton BC, Weisskoff RM. Imaging subcortical auditory activity in humans. *Hum Brain Mapp* 1998;6:33–41. [PubMed: 9673661]
- Hunt SP, Mantyh PW. The molecular dynamics of pain control. *Nat Rev Neurosci* 2001;2:83–91. [PubMed: 11252998]
- Iadarola MJ, Berman KF, Zeffiro TA, Byas-Smith MG, Gracely RH, Max MB, Bennett GJ. Neural activation during acute capsaicin-evoked pain and allodynia assessed with PET. *Brain* 1998;121(Pt 5):931–947. [PubMed: 9619195]
- Jacob CA, Cabral AH, Almeida LP, Magierek V, Ramos PL, Zanoveli JM, Landeira-Fernandez J, Zangrossi H, Nogueira RL. Chronic imipramine enhances 5-HT(1A) and 5-HT(2) receptors-mediated inhibition of panic-like behavior in the rat dorsal periaqueductal gray. *Pharmacol Biochem Behav* 2002;72:761–766. [PubMed: 12062564]
- Koltzenburg M, Lundberg LE, Torebjork HE. Dynamic and static components of mechanical hyperalgesia in human hairy skin. *Pain* 1992;51:207–219. [PubMed: 1484717]
- Lee BH, Park SH, Won R, Park YG, Sohn JH. Antiallodynic effects produced by stimulation of the periaqueductal gray matter in a rat model of neuropathic pain. *Neurosci Lett* 2000;291:29–32. [PubMed: 10962146]
- Lindblom U, Verrillo RT. Sensory functions in chronic neuralgia. *J Neurol Neurosurg Psychiatry* 1979;42:422–435. [PubMed: 448382]
- Lorenz J, Cross D, Minoshima S, Morrow T, Paulson P, Casey K. A unique representation of heat allodynia in the human brain. *Neuron* 2002;35:383–393. [PubMed: 12160755]
- Maihofner C, Neundorfer B, Stefan H, Handwerker HO. Cortical processing of brush-evoked allodynia. *Neuroreport* 2003;14:785–789. [PubMed: 12858033]
- Maihofner C, Schmelz M, Forster C, Neundorfer B, Handwerker HO. Neural activation during experimental allodynia: a functional magnetic resonance imaging study. *Eur J Neurosci* 2004;19:3211–3218. [PubMed: 15217377]
- McMahon SB, Wall PD. Receptive fields of rat lamina 1 projection cells move to incorporate a nearby region of injury. *Pain* 1984;19:235–247. [PubMed: 6089072]
- Ochoa JL, Yarnitsky D. Mechanical hyperalgesias in neuropathic pain patients: dynamic and static subtypes. *Ann Neurol* 1993;33:465–472. [PubMed: 8388678]
- Odeh F, Antal M, Zagon A. Heterogeneous synaptic inputs from the ventrolateral periaqueductal gray matter to neurons responding to somatosensory stimuli in the rostral ventromedial medulla of rats. *Brain Res* 2003;959:287–294. [PubMed: 12493617]
- Ossipov MH, Bian D, Malan TP Jr, Lai J, Porreca F. Lack of involvement of capsaicin-sensitive primary afferents in nerve-ligation injury induced tactile allodynia in rats. *Pain* 1999;79:127–133. [PubMed: 10068158]
- Pertovaara A, Kontinen VK, Kalso EA. Chronic spinal nerve ligation induces changes in response characteristics of nociceptive spinal dorsal horn neurons and in their descending regulation originating in the periaqueductal gray in the rat. *Exp Neurol* 1997;147:428–436. [PubMed: 9344567]
- Petersen KL, Rowbotham MC. A new human experimental pain model: the heat/capsaicin sensitization model. *Neuroreport* 1999;10:1511–1516. [PubMed: 10380972]
- Petrovic P, Ingvar M, Stone-Elander S, Petersson KM, Hansson P. A PET activation study of dynamic mechanical allodynia in patients with mononeuropathy. *Pain* 1999;83:459–470. [PubMed: 10568854]
- Peyron R, Laurent B, Garcia-Larrea L. Functional imaging of brain responses to pain. A review and meta-analysis (2000). *Neurophysiol Clin* 2000;30:263–288. [PubMed: 11126640]
- Porreca F, Lai J, Bian D, Wegert S, Ossipov MH, Eglen RM, Kassotakis L, Novakovic S, Rabert DK, Sangameswaran L, Hunter JC. A comparison of the potential role of the tetrodotoxin-insensitive sodium channels, PN3/SNS and NaN/SNS2, in rat models of chronic pain. *Proc Natl Acad Sci U S A* 1999;96:7640–7644. [PubMed: 10393873]
- Porro CA. Functional imaging and pain: behavior, perception, and modulation. *Neuroscientist* 2003;9:354–369. [PubMed: 14580120]

- Saab CY, Willis WD. The cerebellum: organization, functions and its role in nociception. *Brain Res Brain Res Rev* 2003;42:85–95. [PubMed: 12668291]
- Schweinhardt P, Glynn C, Brooks J, McQuay H, Jack T, Chessell I, Bountra C, Tracey I. An fMRI study of cerebral processing of brush-evoked allodynia in neuropathic pain patients. *Neuroimage*. 2006
- Simone DA, Baumann TK, Collins JG, LaMotte RH. Sensitization of cat dorsal horn neurons to innocuous mechanical stimulation after intradermal injection of capsaicin. *Brain Res* 1989;486:185–189. [PubMed: 2720428]
- Simone DA, Sorkin LS, Oh U, Chung JM, Owens C, LaMotte RH, Willis WD. Neurogenic hyperalgesia: central neural correlates in responses of spinothalamic tract neurons. *J Neurophysiol* 1991;66:228–246. [PubMed: 1919669]
- Suzuki R, Rahman W, Hunt SP, Dickenson AH. Descending facilitatory control of mechanically evoked responses is enhanced in deep dorsal horn neurones following peripheral nerve injury. *Brain Res* 2004a;1019:68–76. [PubMed: 15306240]
- Suzuki R, Rygh LJ, Dickenson AH. Bad news from the brain: descending 5-HT pathways that control spinal pain processing. *Trends Pharmacol Sci* 2004b;25:613–617. [PubMed: 15530638]
- Talairach J, Tournoux P. *Coplanar Stereotaxic Atlas of the Human Brain*, Vol. Stuttgart: Thieme edn. 1988
- Torebjork HE, Lundberg LE, LaMotte RH. Central changes in processing of mechanoreceptive input in capsaicin-induced secondary hyperalgesia in humans. *J Physiol* 1992;448:765–780. [PubMed: 1593489]
- Tracey I, Ploghaus A, Gati JS, Clare S, Smith S, Menon RS, Matthews PM. Imaging attentional modulation of pain in the periaqueductal gray in humans. *J Neurosci* 2002;22:2748–2752. [PubMed: 11923440]
- Urban MO, Gebhart GF. Supraspinal contributions to hyperalgesia. *Proc Natl Acad Sci U S A* 1999;96:7687–7692. [PubMed: 10393881]
- Vanegas H, Schaible HG. Descending control of persistent pain: inhibitory or facilitatory? *Brain Res Brain Res Rev* 2004;46:295–309. [PubMed: 15571771]
- Voisin DL, Guy N, Chalus M, Dallel R. Nociceptive stimulation activates locus coeruleus neurones projecting to the somatosensory thalamus in the rat. *J Physiol* 2005;566:929–937. [PubMed: 15905214]
- Witting N, Kupers RC, Svensson P, Arendt-Nielsen L, Gjedde A, Jensen TS. Experimental brush-evoked allodynia activates posterior parietal cortex. *Neurology* 2001;57:1817–1824. [PubMed: 11723270]
- Woolf CJ, King AE. Dynamic alterations in the cutaneous mechanoreceptive fields of dorsal horn neurons in the rat spinal cord. *J Neurosci* 1990;10:2717–2726. [PubMed: 2388084]
- Woolf CJ, Shortland P, Sivilotti LG. Sensitization of high mechanothreshold superficial dorsal horn and flexor motor neurones following chemosensitive primary afferent activation. *Pain* 1994;58:141–155. [PubMed: 7816483]
- Young RF, Perryman KM. Pathways for orofacial pain sensation in the trigeminal brain-stem nuclear complex of the Macaque monkey. *J Neurosurg* 1984;61:563–568. [PubMed: 6747695]
- Zambreanu L, Wise RG, Brooks JC, Iannetti GD, Tracey I. A role for the brainstem in central sensitisation in humans. Evidence from functional magnetic resonance imaging. *Pain* 2005;114:397–407. [PubMed: 15777865]
- Zhang WT, Mainero C, Kumar A, Wiggins CJ, Benner T, Purdon PL, Bolar DS, Kwong KK, Sorensen AG. Strategies for improving the detection of fMRI activation in trigeminal pathways with cardiac gating. *Neuroimage* 2006;31:1506–1512. [PubMed: 16624588]

Control session*Heat/capsaicin session***Figure 1. Experimental design**

Twelve healthy subjects were randomly assigned to one of two counterbalanced groups to undergo two fMRI sessions, separated by an interval of at least a week, one during innocuous brush to the right ophthalmic division (V1) of the trigeminal nerve immediately after heat/capsaicin-induced allodynia (heat/capsaicin session), and one during the same stimuli to the untreated right V1 (control session). The order of the two sessions was randomized. During the heat/capsaicin session, we first marked in each subject the treatment site on the right V1 (1.6 cm^2). The premarked skin was then heated for 5 minutes at 45°C using a 1.6 cm^2 Peltier thermode (Medoc, Haifa Israel) after which 0.1% of capsaicin cream (Capzasin-HP, Chattem, Inc, USA) was applied over the same area for other 30 minutes. After capsaicin removal, the borders of the area of secondary allodynia were delineated with a brush. Then, during fMRI innocuous mechanical stimuli were administered to the premarked sites of interest (primary area, PA; secondary area, SA) on the right V1. In the control session, the same stimuli were administered to the normal skin of the same cutaneous area.

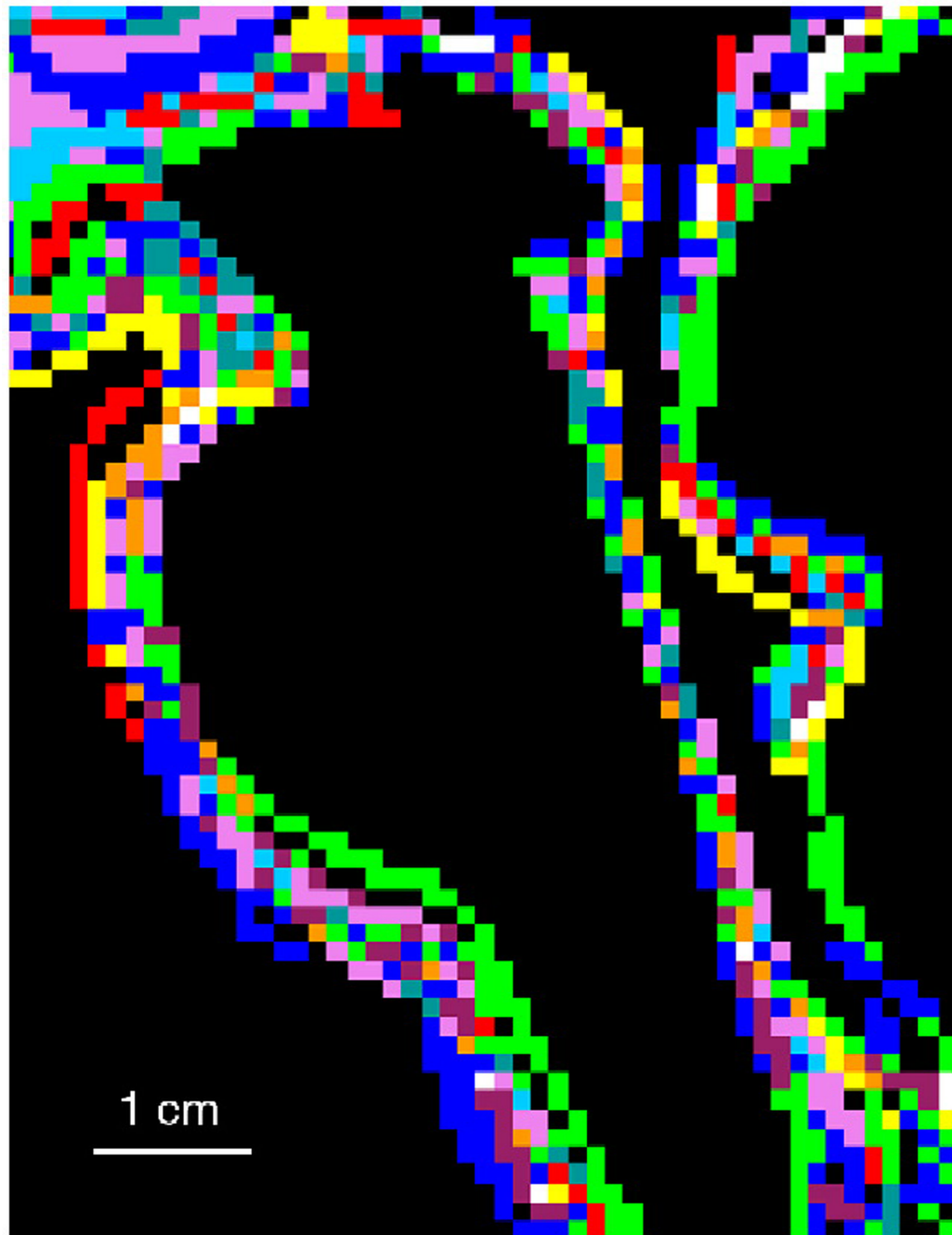


Figure 2. Brainstem anatomical outlines of study subjects

Sagittal view of brainstem anatomical outlines of all study subjects. Individual outlines are displayed in different colors. To quantify the accuracy of brainstem co-registration, we defined in the mid-sagittal plane the angle between the line connecting the anterior and posterior commissure and the line connecting the posterior commissure and the obex in the medulla. The angles of all subjects ranged from 112.17 to 115.68 degrees (114.02 ± 1.19 , mean \pm SD), which corresponds to the SD of 1–1.5 mm at the obex.

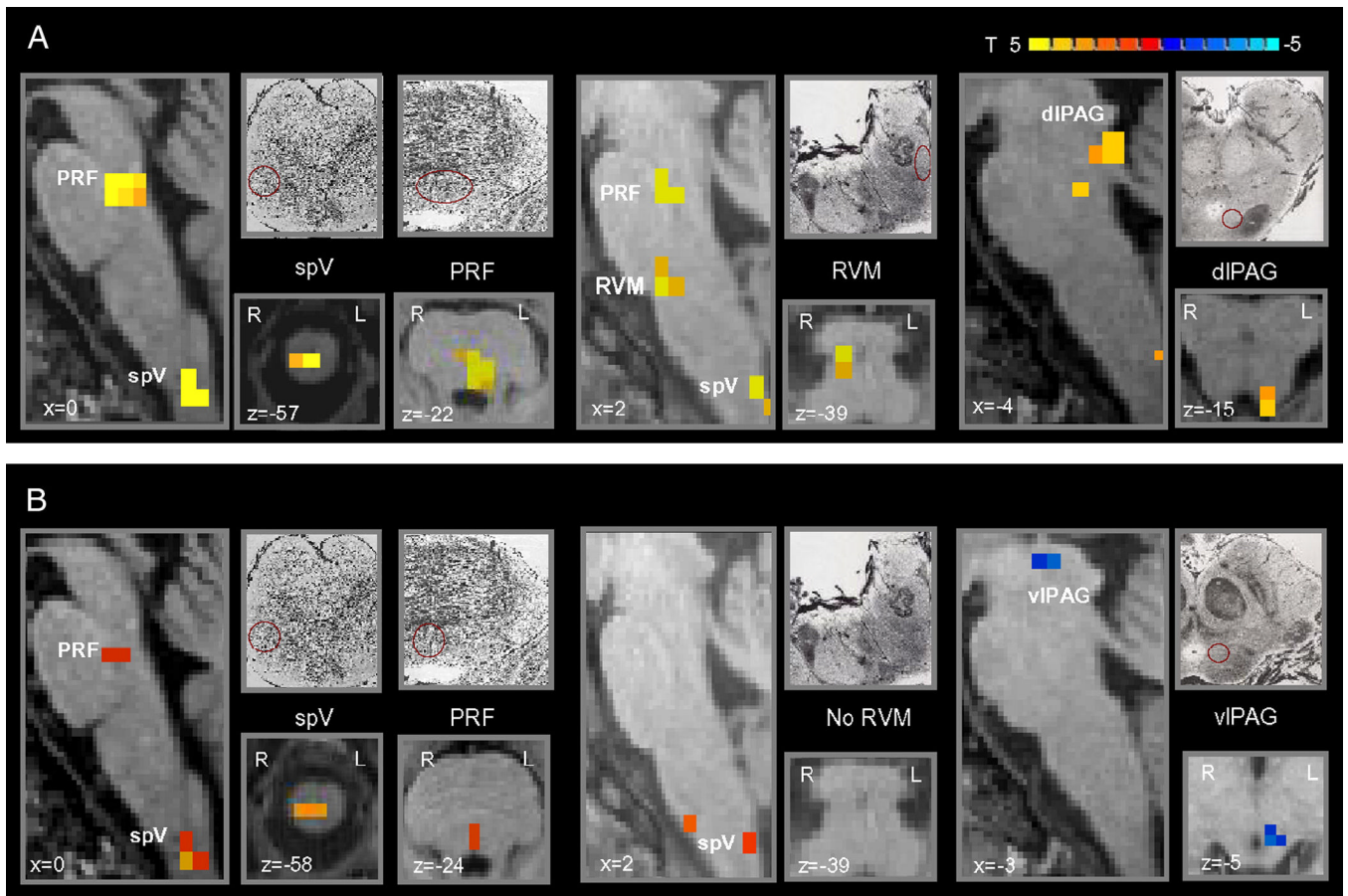


Figure 3. Brainstem differences of brush to either the primary or secondary area versus the normal skin

Group statistical comparison t maps (radiological convention; $p < 0.05$, corrected), overlaid on high resolution anatomical images in Talairach space, showing in 11 healthy subjects significant differences in the brainstem during brush to either (A) the primary or (B) secondary area following heat/capsaicin application to the right ophthalmic division of the trigeminal nerve versus brush to the untreated skin of the same cutaneous territory. Sketches and micrographs adapted from the atlas of Duvernoy (1995) were used to help identify the location of activation clusters.

(spV = spinal trigeminal nucleus; PRF = pons reticular formation; RVM = rostroventromedial medulla; dIPAG = dorsolateral PAG; vlPAG = ventrolateral PAG).

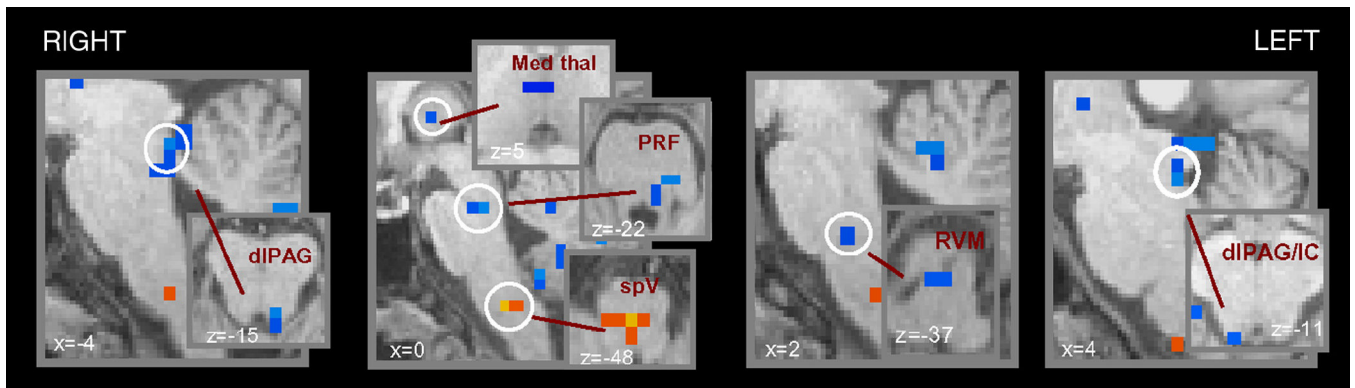


Figure 4. Brainstem differences of brush to the secondary area versus brush to the primary area Group statistical comparison t maps (radiological convention; $p < 0.05$, corrected), overlaid on high resolution anatomical images in Talairach space, showing in 11 healthy subjects significant differences in the brainstem during brush to either secondary area versus brush to the primary following heat/capsaicin application to the right ophthalmic division of the trigeminal nerve versus brush to the untreated skin of the same cutaneous territory. In blue are represented the clusters more activated during primary versus secondary dynamic mechanical allodynia, the opposite is true for the activation in the caudal medulla shown in yellow/red.

(MRF = medulla reticular formation; PRF = pons reticular formation; dIPAG = dorsolateral PAG; Med Thal = medial thalamus; IC = inferior colliculus).

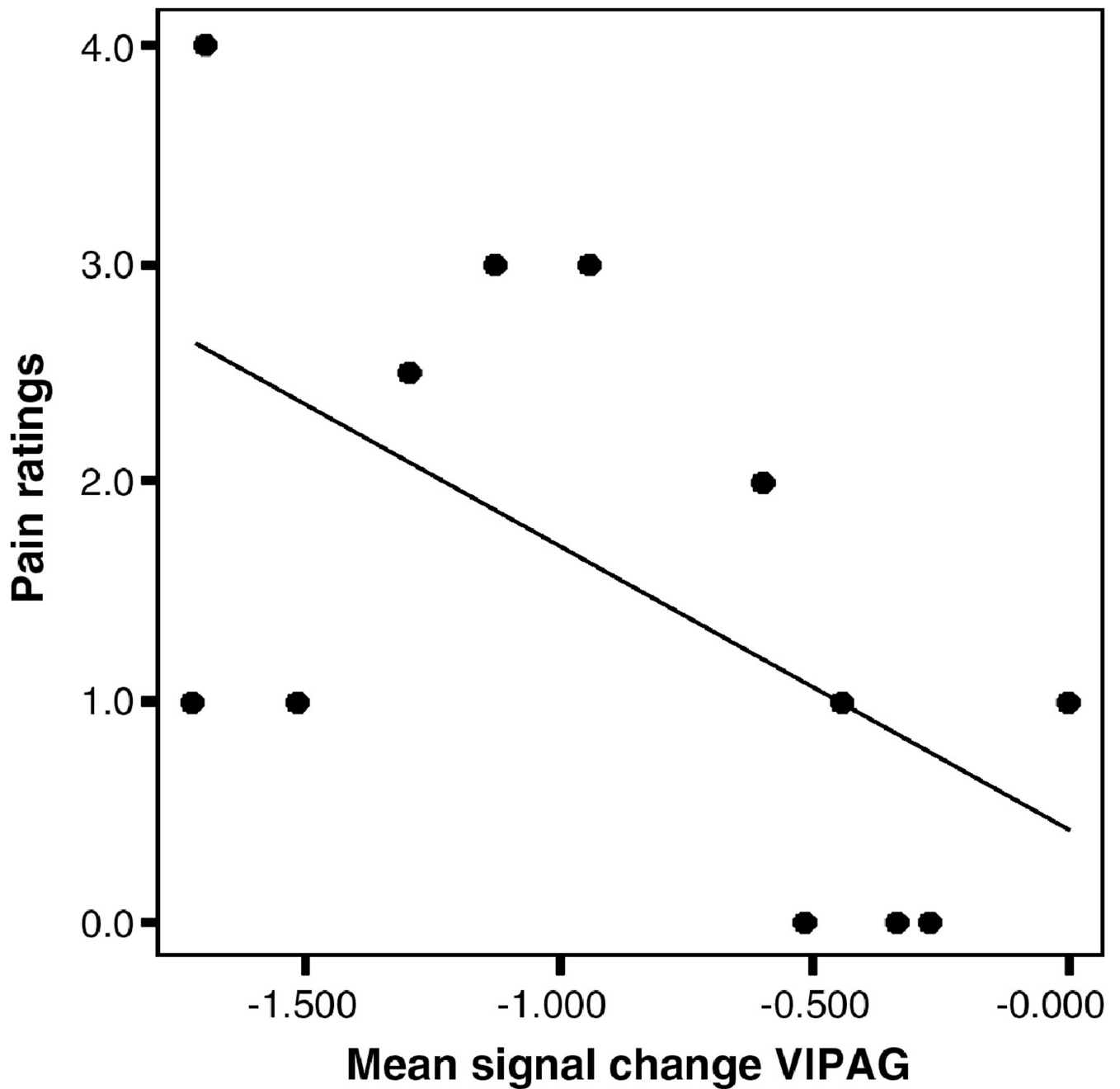


Figure 5. Correlation between the mean signal change in the contralateral ventrolateral periaqueductal gray and pain intensity ratings during primary mechanical allodynia
Correlation analysis showing a significant inverse correlation ($p < 0.05$, Pearson's correlation coefficient = -0.6) between the mean signal change in the contralateral ventrolateral periaqueductal gray and pain intensity ratings during primary dynamic mechanical allodynia, i.e. the more deactivated the VIPAG the higher the pain intensity.

Table 1

Significant differences between brush to either the primary or secondary area following heat/capsaicin application to the right ophthalmic division (V1) of the trigeminal nerve and the same stimulus to the same untreated skin area in 11 healthy subjects.

Area	Brush to the primary area vs brush to the untreated skin (right V1)		Brush to the secondary area vs brush to the untreated skin (right V1)	
	Talairach x, y, z	T	Talairach x, y, z	T
Ipsi Dorsal Medu (spV)	1, -41, -58	4.16	0, -42, -57	2.70
Ventral Medulla (RVM)	3, -25, -40	2.57		
Pons Reticular Formation	0, 26, -23	4.2	-1, -28, -24	2.00*
Ctrl PAG	-4, -34, -13	2.50	-4, -25, -4	-2.90**
Ipsi Amygdala			12, -5, -21	2.49
Ctrl Amygdala	-28, -8, -9	2.31		
Ipsi Lateral Thal	17, -11, 4	4.02		
Ctrl Lateral Thal	-13, -13, 15	2.61		
Ctrl Medial Thal	-4, -1, 2, 7	3.07		
Ipsi Caudate	19, 13, 9	2.75		
Ipsi Insula			28, 14, 5	2.96
Ipsi Ant Cingulate (BA 32/23)	1, -12, 28	3.79	3, 27, 32	2.63
Ctrl Ant Cingulate (BA 32)	-8, 13, 37	2.91		
	-1, -11, 29	2.41		
Ipsi SMA (BA 6)	5, -11, 57	2.92	5, -10, 57	2.53
Ctrl SMA (BA 6)	-6, -16, 61	3.32		
Ipsi LPS (BA 7/5)	20, -45, 65	3.39	20, -45, 65	2.70
			15, -38, 65	2.61
Ctrl LPS (BA 7/5)	-13, -40, 61	2.55	-21, -46, 65	2.36
Vermis	9, -49, -9	2.48	-6, -65, -24	2.41

T = maximum *t*

* $p < 0.01$, uncorrected

** minimum *t* (decreased activation); Ipsi = ipsilateral; Ctrl = contralateral; spV = spinal trigeminal nucleus; RVM = rostroventromedial medulla; PAG = periaqueductal gray; Thal = thalamus; LPS = superior parietal lobule; SMA = supplementary motor area; Ant = anterior; Post = posterior; Sup = superior.

Table 2

Significant differences in the brainstem and thalamus between secondary and primary dynamic mechanical allodynia to the right ophthalmic division (V1) of the trigeminal nerve of 11 healthy subjects.

Area	Brush to the secondary area vs brush to the primary area (right V1)	
	Talairach x, y, z	T
Medulla Reticular Formation	0, -30, -49	2.60
Ventral Medulla (RVM)	0, -25, -37	-2.22*
Pons Reticular Formation	-1, -24, -21	-2.51*
Ipsi dIPAG/IC	5, -32, -12	-2.94*
Ctrl dIPAG	-4, -32, -15	-2.23*
Ipsi Medial Thal	5, -10, 5	-2.28*
Ctrl Ant Cingulate (BA 24)	-8, 31, 9	-2.83*
Ctrl Post Cingulate (BA 23/30)	-5, -53, 20	-5.24*
Ctrl Sup Frontal Gyrus (BA 9)	-4, 53, 32	-2.31*
Ctrl Sup Frontal Gyrus (BA 8)	-13, 26, 54	-4.35*
Ipsi Cerebellum	1, -41, -18	-3.03*
Ctrl Cerebellum	-34, -57, -49	-3.27*

T = maximum *t*

* minimum *t* (deactivation); Ipsi = ipsilateral; Ctrl = contralateral; spV = spinal trigeminal nucleus; RVM = rostroventromedial medulla; dIPAG = dorsolateral periaqueductal gray; IC = inferior colliculus; Thal = thalamus; Ant = anterior; Post = posterior; Sup = superior.